A conformational and vibrational study of $CF_3COSCH_2CH_3$

María Eliana Defonsi Lestard,[1] María Eugenia Tuttolomondo,[1] Derek A. Wann,[2] Heather E. Robertson,[2] David W. H. Rankin,[2] and Aida Ben Altabef[1,a)]
[1]*Instituto de Química del Noroeste Argentino (INQUINOA), Consejo Nacional de Investigaciones Científicas y Técnicas (CONICET), Argentina and Instituto de Química Física, Facultad de Bioquímica, Química y Farmacia, Universidad Nacional de Tucumán, San Lorenzo 456, T4000CAN Tucumán, Argentina*
[2]*School of Chemistry, University of Edinburgh, West Mains Road, Edinburgh EH9 3JJ, United Kingdom*

(Received 22 July 2009; accepted 4 November 2009; published online 3 December 2009)

The molecular structure and conformational properties of *S*-ethyl trifluorothioacetate, $CF_3COSCH_2CH_3$, were determined in the gas phase by electron diffraction and vibrational spectroscopy (IR and Raman). The experimental investigations were supplemented by *ab initio* (Møller Plesset of second order) and density functional theory quantum chemical calculations at different levels of theory. Both experimental and theoretical methods reveal two structures with C_s (*anti*, *anti*) and C_1 (*anti*, *gauche*) symmetries, although there are disagreements about which is more stable. The electron diffraction intensities are best interpreted with a mixture of 51(3)% *anti*, *anti* and 49(3)% *anti*, *gauche* conformers. This conformational preference was studied using the total energy scheme and the natural bond orbital scheme. In addition, the infrared spectra of $CF_3COSCH_2CH_3$ are reported for the gas, liquid and solid phases as well as the Raman spectrum of the liquid. Using calculated frequencies as a guide, evidence for both C_s and C_1 structures is obtained in the IR spectra. Harmonic vibrational frequencies and scaled force fields have been calculated for both conformers. © *2009 American Institute of Physics*. [doi:10.1063/1.3267633]

I. INTRODUCTION

S-ethyl trifluorothioacetate, $CF_3COSCH_2CH_3$, is a trifluoroacetylating agent used to provide an amine-protecting group.[1] The intense electrophilic nature of the trifluoroacyl group combined with the unusual aminophilicity of the sulfur atom makes it ideal for use in peptide syntheses.[2] Thioesters such as $CF_3COSCH_2CH_3$ are also important components of coenzyme A, which plays an essential role in metabolism. The microwave spectra of several ethyl thioesters were reported by True *et al.* in 1981,[3] though notably they determined the existence of only one stable conformer of the title molecule.

Our previous studies of various esters of trifluoroacetic acid with the general formula CF_3CO_2R (Refs. 4–6) (R $=CH_3$, CH_2CH_3, CH_2CF_3) have therefore been extended to include the related thioester, $CF_3COSCH_2CH_3$, the first of the type CF_3COXR. Although the structural and conformational properties of simple oxoesters and thioesters have been studied by several groups mainly because of the central role of thioesters in the metabolic process, the factors controlling this behavior are far from being understood. This was highlighted in an extensive computational study undertaken by Drueckhammer *et al.*[7] The role played by experimental structural studies in understanding the behavior of molecules has been recently discussed,[8] and gas electron diffraction (GED) has already been used to determine the structures of many —SC═O— containing compounds. In addition to the early work of Shen and Hagen on ClC(O)SCl,[9] the GED group of Oberhammer *et al.* reported gas-phase structures for several related species.[10–15]

Here we investigate the characteristic conformations and force constants of $CF_3COSCH_2CH_3$; the comparison of the conformations and geometrical parameters with those of $CF_3CO_2CH_2CH_3$ (Ref. 5) is particularly interesting. We have determined the structure of the molecule using GED, and additionally, infrared and Raman spectra have been recorded for different physical states and the molecular structures and vibrational wavenumbers of the different conformers were calculated quantum mechanically. The spectral features were subsequently assigned to the different normal modes of vibration. The study was complemented by natural bond orbital (NBO) analysis to assess the significance of hyperconjugative interactions, which would favor one conformation over another.

II. EXPERIMENTAL

Samples of $CF_3COSCH_2CH_3$ for use in both electron diffraction and spectroscopy experiments were purchased from Sigma-Aldrich and used without further purification. All handling was performed under dry nitrogen to protect the samples from atmospheric humidity.

A. Infrared and raman spectroscopy

Infrared spectra for $CF_3COSCH_2CH_3$ in the liquid and solid phases were recorded in the 4000–400 cm^{-1} range at room temperature using a Perkin-Elmer GX1 Fourier transform infrared instrument. A glass cell with a 10 cm optical path and Si windows was used to obtain the gas-phase spec-

a)Author to whom correspondence should be addressed. Tel.: +54-381-4311044. FAX: +54-381-4248169. Electronic mail: altabef@fbqf.unt.edu.ar. Member of the Carrera del Investigador Científico, CONICET, Argentina.

tra. The spectrum for the solid was obtained after depositing the compound from the vacuum line onto a KBr window, maintained at about 197 K, in a variable temperature RIIC (VLT-2) cell. Raman spectra of the liquid at room temperature, polarized at 0° and 90°, were obtained with a Fourier Transform-Raman RFS 100/S spectrometer using 1064 nm light from an Nd-YAG (Neodymium-doped yttrium aluminum garnet) laser for excitation.

B. GED

Data were collected for $CF_3COSCH_2CH_3$ on Kodak Electron Image films using the Edinburgh GED apparatus.[16] The accelerating voltage was held at approximately 40 keV, yielding electrons with a wavelength of approximately 6 pm. Data were collected at two nozzle-to-film distances to increase the range of angles over which scattering was observed. The nozzle was at room temperature (approximately 293 K), while the sample was cooled to 253 K for both experiments.

The scattering patterns were converted into digital form using an Epson Expression 1680 Pro flatbed scanner and an extraction program described elsewhere.[17] Data reduction and least-squares refinements were performed using the ED@ED V.3.0 program[18] employing the scattering factors of Ross *et al.*[19] The weighting points for the off-diagonal weight matrices, correlation parameters, and scale factors for both nozzle-to-film distances are given in Table S1.[20]

C. Computational details

Calculations were performed using the resources of the United Kingdom National Service for Computational Chemistry Software (NSCCS),[21] running the GAUSSIAN 03 suite of programs.[22] Potential-energy curves were calculated at the MP2, mPW1PW91, and B3LYP levels using the 6-31G(d), 6-311G(d,p), and 6-311++G(d,p) basis sets, as well as using the B3LYP/6-311G(3df,3dp) combination, and two minima were identified by rotating about the S—C(H_2) bond. All calculations were performed in such a way that only the given torsion was fixed and all other parameters were allowed to relax. The total energy curve was constructed in steps of 5° or 10° using default convergence criteria as implemented in GAUSSIAN 03.[22]

The minima related to one C_s-symmetric structure and one with C_1 symmetry. The difference in total energy between the two minima was small. The calculations showed that only structures with staggered CH_3 and CF_3 groups were real.

Geometry optimizations were performed for both conformers at the MP2 (Ref. 23) and density functional theory (DFT) methods with the 6-311G(d),[24] 6-311G(3df,3pd),[25–27] and 6-311++G(d,p) (Ref. 28) basis sets. One of the DFT methods used Becke's B3 (Ref. 18) hybrid exchange functional and the Lee–Yang–Parr nonlocal correlation functional (LYP).[29] The second DFT method was mPW1PW91, which used a modified Perdew–Wang exchange functional and Perdew–Wang 91 correlation functional.[30] All calculations were spin-restricted and frozen-core. At the B3LYP/6-311++G(d,p) level, the free energies of the two conformers were calculated, showing that the C_s-symmetric conformer was lower in energy than the C_1 conformer by approximately 2.6 kJ mol^{-1}.

Vibrational frequencies were calculated from analytic second derivatives to check that optimized structures represented minima on the potential-energy surface. Force constants calculated at the B3LYP/6-311++G(d,p) level were subsequently used, along with the program SHRINK,[31] to obtain initial amplitudes of vibration and also to calculate curvilinear distance correction terms for use in the GED refinement. The structure obtained from the refinement is therefore of the type r_{h1}. A NBO calculation was performed at the B3LYP/6-311++G(d,p) level using the NBO 3.0 code[32] as implemented in the GAUSSIAN 03 package.[22]

A harmonic force field in Cartesian coordinates calculated at the B3LYP/6-311++G(d,p) level was transformed to a set of natural internal (local symmetry) coordinates[33] via the B matrix[34] using a standard program. The scaled quantum mechanical (SQM) force field was obtained using the scheme outlined by Pulay *et al.*,[35] in which the diagonal force constants are multiplied by scale factors $f_i, f_j, \ldots$, and the corresponding interaction constants are multiplied by $(f_i f_j)^{1/2}$, thus adjusting the scale factors to reproduce the experimental frequencies as well as possible. An initial set of scale factors was refined to fit the calculated frequencies to the experimental data. No empirical correction of the theoretical geometry was used. The potential-energy distribution was then calculated with the resulting SQM force field. The force field for the C_s conformation, scaling, and determination of the potential-energy distribution were performed with the program FCARTP.[36] The atomic displacements given by the GAUSSIAN 03 program for each vibrational mode were used to understand the nature of the molecular vibrations qualitatively, and for that purpose, the corresponding data were represented graphically using the GAUSSVIEW program.[37]

III. RESULTS AND DISCUSSION

A. Quantum chemical calculations

Two stable conformations, with C_1 (*anti*, *gauche*) and C_s (*anti*, *anti*) symmetries (Fig. 1), were identified with every combination of theory and basis set that was used. In the *anti*, *anti* conformation [Fig. 1(b)], the C(15)C(16)S(28)C(21) and C(16)S(28)C(21)C(24) dihedral angles are both 180°. In the *anti*, *gauche* conformations (two enantiomeric forms), the C(1)C(2)S(14)C(7) dihedral angles are 180°, while the C(2)S(14)C(7)C(10) dihedral angle has a *gauche* value of approximately +/−80°.

Calculated geometrical parameters for $CF_3COSCH_2CH_3$ are listed in Table I along with parameters from the experimental electron diffraction structure. As was found for the related compound $CH_3SO_2SCH_3$,[38] the inclusion of extra polarization functions (beyond a single d function) is necessary to predict the bond lengths in this type of molecule accurately. The parameter most sensitive to this orbital description is the X—S bond, which was shortened by 1.4 pm. upon replacing the 6-311G(d) basis set with 6-311G(3df,3pd). All bonds involving the sulfur atom were

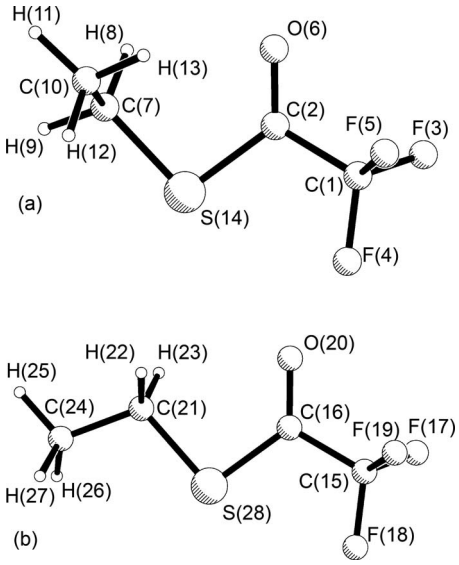

FIG. 1. Molecular structures (including atom numbering used in the GED refinement) of (a) the C_1 conformer and (b) the C_s conformer of $CF_3COSCH_2CH_3$.

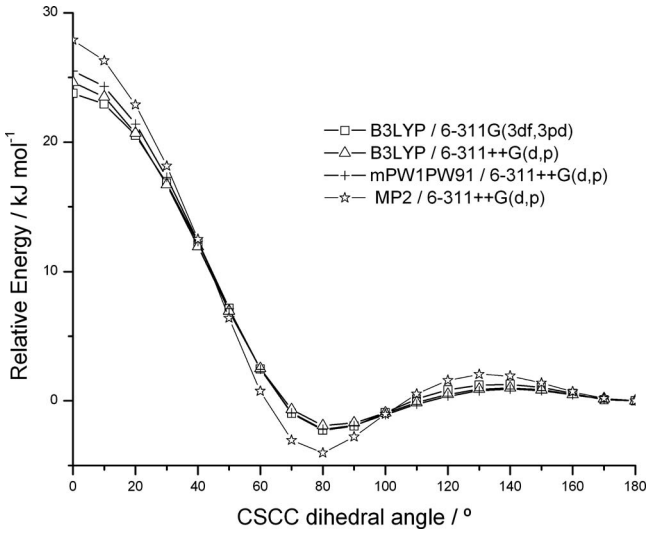

FIG. 2. Torsional potential about the S–C(H_2) bond of $CF_3COSCH_2CH_3$ calculated at MP2, mPW1PW91, and B3LYP levels using the 6-311++G(d,p) basis set.

shortened by over 1 pm., but the remaining bond lengths were relatively unchanged. An additional geometry optimization was performed with the 6-311G(d) basis on all atoms except the sulfur atom, for which a 6-311G(3df) basis set was used. This produced a geometry close to both the experimental structure and to that calculated using the 6-311G(3df,3pd) basis set, demonstrating that only the polarization of the basis set on sulfur is critical for obtaining accurate bond lengths in these types of structures. (See Table S2 for the root-mean-square deviations (RMSD) between the GED distances and some calculated ones.)[20]

In 1981 True *et al.*[3] measured the barrier to rotation about the CSCC dihedral angle in $CF_3COSCH_2CH_3$ using microwave spectroscopy. The barrier height was found to be 5.85 kJ mol^{-1}, which differs significantly from the computed results quoted in this work. The same microwave spectroscopic study determined the presence of only one conformer (the *anti*, *gauche* structure) rather than the two conformers identified by our calculations and evident in the GED and vibrational spectroscopy results. Studying the nature of the CSCC barrier is extremely interesting as we will be able to find the two conformations reported by GED and the causes of their stability.

The potential-energy scans about the S—C(H_2) bond at the MP2, mPW1PW91, and B3LYP levels using the 6-311++G(d,p) basis set and using the B3LYP/6-311G(3df,3pd) combination are shown in Fig. 2. There is good agreement between methods, identifying two stable forms, one with C_1 symmetry and another with C_s symmetry. The total and rela-

TABLE I. Selected calculated and experimental (GED) geometrical parameters for $CF_3COSCH_2CH_3$ and $CF_3CO_2CH_2CH_3$.

	$CF_3COSCH_2CH_3$				$CF_3CO_2CH_2CH_3$[a]			
	C_s conformer		C_1 conformer		C_s conformer		C_1 conformer	
Geometrical parameter[b]	GED	Calculated[c]	GED	Calculated[c]	GED	Calculated[c]	GED	Calculated[c]
Distances								
C(15)—F mean	134.0	133.8	134.0	133.7	134.4	134.2	133.8	134.2
C(15)—C(16)	154.6	154.6	154.6	154.6	154.5	154.3	154.6	154.4
C(16)=O(20)	121.6	121.4	121.6	121.4	121.2	120.6	121.3	120.7
C(16)—S/O(28)	175.9	175.0	176.1	175.2	133.1	133.0	133.0	132.9
S/O(28)—C(21)	182.7	181.5	182.6	181.5	145.4	145.1	145.6	145.5
C(21)—C(24)	153.3	152.6	153.2	152.5	150.8	151.2	151.2	151.6
Angles								
C(15)—C(16)—S/O(28)	114.3	115.2	113.7	114.6	110.1	109.6	110.1	109.4
C(16)—S/O(28)—C(21)	95.9	97.4	95.9	97.6	114.6	114.7	115.1	115.4
S/O(28)—C(21)—C(24)	111.3	109.3	115.0	112.8	104.4	106.9	109.3	110.7
Dihedral angles								
C(15)—C(16)—S/O(28)—C(21)	180.0	180.0	161.4	173.8	180.0	180.0	182.4	179.9
C(16)—S/O(28)—C(21)—C(24)	180.0	180.0	−78.0	−78.4	180.0	180.0	98.7	86.0

[a]Reference 4.
[b]Distances in picometer and angles in degrees.
[c]MP2/6-311++G(d,p).

TABLE II. Free energies (zero-point corrected), differences in free energies (energies in hartrees), and differences in total energies (not zero-point corrected) for two conformers of $CF_3COSCH_2CH_3$ at different levels of theory.

Method	Basis set	$G(C_1)$	$G(C_s)$	ΔE_T (kJ mol^{-1})	ΔG^a (kJ mol^{-1})	Barrier height[b] (kJ mol^{-1})
B3LYP	6-31G(d)	−928.318 21	−928.318 20	−1.93	−0.03	25.57
	6-311G(d,p)	−928.504 02	−928.503 88	−2.83	−0.36	26.55
	6-311G(3df,3dp)	−928.551 07	−928.551 08	−2.15	0.03	23.79
	6-311++G(d,p)	−928.519 62	−928.520 61	−2.07	2.60	26.52
MP2	6-31G(d)	−926.346 79	−926.346 52	−3.58	−0.71	30.37
	6-311++G(d,p)	−926.716 74	−926.713 75	−4.10	−7.85	31.92
mPW1PW91	6-31G(d)	−928.199 55	−928.199 52	−2.03	−1.15	26.88
	6-311G(d,p)	−928.374 32	−928.374 21	−3.09	−0.31	27.90
	6-311++G(d,p)	−928.388 67	−928.388 77	−2.21	0.27	27.51
Experimental[c]						5.85

[a] $\Delta G = G(C_1) - G(C_s)$.
[b] $\Delta G = E_T(TS) - E_T(C_1)$.
[c] Value from the microwave study in Ref. 3.

tive energies of the conformers given by various calculations are listed in Table II. At the MP2/6-311++G(d,p) level the free energies of the two conformers showed that the C_1-symmetric conformer was lower in energy than the C_s conformer by approximately 7.85 kJ mol^{-1}; at the B3LYP/6-311++G(d,p) level the corresponding energy difference was 2.60 kJ mol^{-1}, with the C_s conformer lower in energy. There is therefore significant disagreement as to the composition of the gas-phase sample that should be determined experimentally by GED.

For both of the conformers identified above, the free energy calculated using the B3LYP/6-311++G(d,p) method was used along with the average temperature of the experiment to estimate (using the Boltzmann distribution) the amount of each conformer that should be observed in the gas phase. As the difference in free energy was calculated to be 2.60 kJ mol^{-1} (C_s conformer lower in energy) and as the C_1 conformer has a double multiplicity relative to the C_s conformer, the ratio of C_1 to C_s conformers was predicted to be 0.41:0.59.

In order to investigate the energetic consequences of rotating about the S—C(H_2) bond, the torsional barrier has been characterized using two different schemes. In the first one, the NBO partitioning scheme has been applied in order to decompose the total energy into the E_{Lewis} and E_{deloc} terms. In the second one, the total energy changes have been decomposed as a sum of potential and kinetic contributions. MP2/6-311++G(d,p) and B3LYP/6-311++G(d,p) have been selected as representative of the methods used in this work for the energy decomposition as they yield good results for barrier height and molecular geometry, respectively. Because the results from the two methods for the selected levels are similar, we will concentrate our discussion on B3LYP/6-311++G(d,p). Plots for HF/6-311++G(d,p) and MP2/6-311++G(d,p) appear as Figures S1 and S2, respectively.[20]

B. Contributions of the lewis and delocalization energies to the barrier

NBO analysis has frequently been used in the evaluation of the anomeric effect and the origin of the internal rotation barrier. NBO analysis allows us to estimate the energy of the molecule with the same geometry but in the absence of the electronic delocalization. Moreover, only the steric and electrostatic interactions through the term E_{Lewis} are taken into account.[39–42]

Following this scheme, the energy barrier $\Delta E_{barrier}$ can be written as a function of bond strength, hyperconjugation, and steric repulsion,

$$\Delta E_{barrier} = \Delta E_{Lewis} + \Delta E_{deloc} = \Delta E_{struct} + \Delta E_{exc} + \Delta E_{deloc}, \quad (1)$$

where ΔE_{struct} takes into account Coulombic and bond-energy changes in the classical structure, ΔE_{exc} [known as the Pauli exchange (or steric) repulsion energy] accounts for the non-Coulombic energy changes arising from the Pauli exclusion principle, and ΔE_{deloc} describes the hyperconjugative stabilization.

Table S3 (Ref. 20) presents the contributions from the localized electron density (E_{Lewis}) and the delocalized electron density (E_{deloc}) to the rotation barrier about the S—C(H_2) bond at the B3LYP/6-311++G(d,p) level. This table shows that the Lewis energy is decisive for the energetic preference; its minima correspond to the *anti*, *anti* and *anti*, *gauche* conformers. When electronic delocalization is lacking, the steric effect would be dominant in both conformers but greater in the *anti*, *anti* conformer as expected for an anomeric effect of stereoelectronic origin (Fig. 3).

The delocalization energy difference, ΔE_{deloc}, is greater for the *anti*, *anti* conformer than for the *anti*, *gauche* conformer. This effect of the *anti*, *gauche* structure in $CF_3COSCH_2CH_3$ can be rationalized by orbital interactions between the two sulfur lone pairs (lp S) and the vicinal antibonding orbitals. According to an NBO analysis, the anomeric orbital interaction lp S(14/28) $\rightarrow \sigma^*$C(7/21)—C(10/24), which only appears in the *anti*, *gauche* form, is 14.92 kJ mol^{-1} (see Table S4).[20]

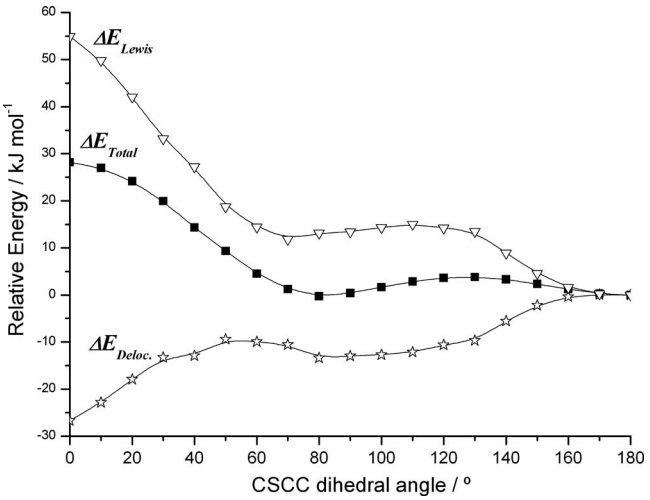

FIG. 3. Dependence of the relative total energy of the $CF_3COSCH_2CH_3$ molecule and its ΔE_{Lewis} and ΔE_{deloc} parts on the CSCC rotation angle calculated using the B3LYP/6-311++G(d,p) method.

C. Contribution of different potential-energy terms to the barrier

In our second approach, we have performed an investigation of the energy barrier based on the partition offered by the scheme,

$$\Delta E = \Delta E_{\text{nn}} + \Delta E_{\text{en}} + \Delta E_{\text{ee}} + \Delta E_{\text{k}}, \tag{2}$$

where ΔE is the total energy change between structures of different geometries, ΔE_{nn} is the energy change for nuclear repulsion, ΔE_{en} is the change in electronic-nuclear attraction energy, ΔE_{ee} is the change in electron repulsion, and ΔE_{k} is the change in kinetic energy. It can be seen that this equation describes the total energy change as a sum of all potential and kinetic contributions.

Table S5 (Ref. 20) illustrates the fact that the repulsive terms, E_{ee} and E_{nn}, are smallest in the *most stable* conformation and that they increase when going to the top of the barrier, while the attractive term E_{en} favors the *anti*, *gauche* (C_1) conformer. More detailed results for the energy as a function of the CSCC torsion are shown in Fig. 4.

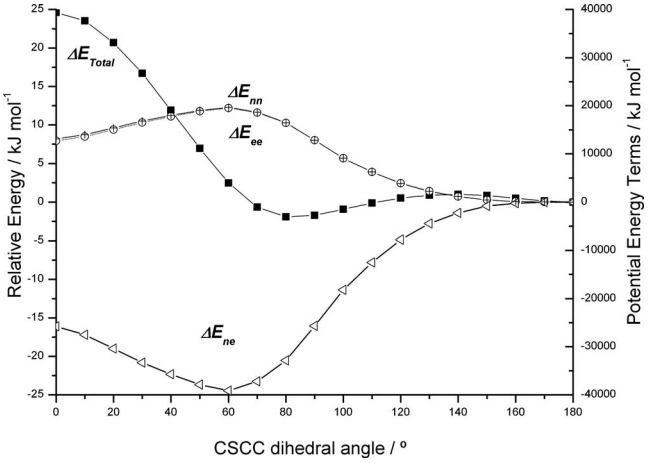

FIG. 4. Dependence of attractive (ΔE_{ne}) and repulsive (ΔE_{nn} and ΔE_{ee}) energy increments on the CSCC dihedral angle in $CF_3COSCH_2CH_3$ calculated at the B3LYP/6-311++G(d,p) level.

The relative stabilization of the C_s conformer could be interpreted as a repulsive interaction between the lone pairs on sulfur and the electronic charge of the C(7/21)—C(10/24) bond, which is minimized when the symmetry is C_s. This is commensurate with the fact that the repulsive terms, E_{ee} and E_{nn}, are smaller in the C_s conformer. The lone pairs, named lp(1) and lp(2), on the S atom are considerably more stable in the C_s conformer than in the C_1 conformer. The same trend is observed for the σ[C(7/21)—C(10/24)] bond orbitals and their antibonding counterparts. The energies and occupancies of the NBOs are listed in Table S6.[20]

IV. GED STUDY

On the basis of the calculations described above [MP2/6-311++G(d,p)], a two-conformer model was written (conformer 1 with C_1 symmetry and conformer 2 with C_s symmetry), describing both geometries in terms of 36 refinable parameters, comprising eight bond lengths and differences, 24 angles and differences, and four dihedral angles (for conformer 1 only). One extra parameter was included (see Table III) to allow the proportion of each conformer present in the mixture to be altered. The atom numbering used in the descriptions of the parameters is shown in Fig. 1.

All C—F, C=O, and C—C distances for both conformers were combined to give an overall average value, and the individual distances (averaged across the two conformers) were described using combinations of differences. The very small differences between the values of these distances in the two conformers were described within the model using parameters that were fixed at calculated values and not allowed to refine. The averages and differences were defined as follows:

$$\begin{aligned} p_1 = \{&[\text{C}(2/16)=\text{O}(6/20)_{\text{mean}}] \\ &+ [\text{C}(1/15)-\text{F}(4/18)_{\text{mean}}] \\ &+ 2[\text{C}(1/15)-\text{F}(3/5/17/19)_{\text{mean}}] \\ &+ [\text{C}(7/21)-\text{C}(10/24)_{\text{mean}}] \\ &+ [\text{C}(1/15)-\text{C}(2/16)_{\text{mean}}]\}/6, \end{aligned}$$

$$\begin{aligned} p_2 = &[\text{C}(1/15)-\text{C}(2/16)_{\text{mean}}] \\ &- \{[\text{C}(2/16)=\text{O}(6/20)_{\text{mean}}] \\ &+ [\text{C}(1/15)-\text{F}(4/18)_{\text{mean}}] \\ &+ 2[\text{C}(1/15)-\text{F}(3/5/17/19)_{\text{mean}}] \\ &+ [\text{C}(7/21)-\text{C}(10/24)_{\text{mean}}]\}/5, \end{aligned}$$

$$\begin{aligned} p_3 = &[\text{C}(7/21)-\text{C}(10/24)_{\text{mean}}] \\ &- \{[\text{C}(2/16)=\text{O}(6/20)_{\text{mean}}] \\ &+ [\text{C}(1/15)-\text{F}(4/18)_{\text{mean}}] \\ &+ 2[\text{C}(1/15)-\text{F}(3/5/17/19)_{\text{mean}}]\}/4, \end{aligned}$$

TABLE III. Refined (r_{h1}) and calculated [refers to MP2/6-311++G(d,p) calculations] (r_e) geometrical parameters for $CF_3COSCH_2CH_3$ from the GED study. [Distances (r) are in pm, and angles ($\angle$) are in degrees. See text for parameter definitions and Fig. 1 for atom numbering. The figures in parentheses are the estimated standard deviations of the last digits. Conformer 1 has C_1 symmetry, and conformer 2 has C_s symmetry.]

	Parameter	r_{h1}	r_e	Restraint
Independent				
p_1	rCF/CO/CC average	138.58(12)	138.29	···
p_2	rCF/CO/CC difference 1	19.24(35)	19.57	19.57(50)
p_3	rCF/CO/CC difference 2	22.29(43)	21.90	21.90(50)
p_4	rCF/CO/CC difference 3	6.21(39)	5.90	5.90(50)
p_5	rCF/CO/CC difference 4	12.52(41)	12.60	12.60(50)
p_6	rCS average	179.30(14)	178.33	···
p_7	rCS difference	−6.69(50)	−6.45	−6.45(50)
p_8	rCH mean	109.6(6)	109.2	109.2(7)
p_9	∠CCH average	112.6(10)	110.6	110.6(10)
p_{10}	∠CCH difference 1	−0.3(5)	−0.3	−0.3(5)
p_{11}	∠CCH difference 2	−1.0(5)	−1.1	−1.1(5)
p_{12}	∠CCH difference 3	0.2(5)	0.2	0.2(5)
p_{13}	∠CCH difference 4	−1.9(5)	−2.1	−2.1(5)
p_{14}	∠H(11)C(10)H(13)	108.2(9)	108.2	108.2(8)
p_{15}	∠H(11)C(10)H(12)	108.5(9)	108.4	108.4(8)
p_{16}	∠H(25)C(24)H(26/27)	108.2(9)	108.1	108.1(8)
p_{17}	∠CSC mean	95.9(6)	97.5	97.5(10)
p_{18}	∠SCC(F_3) average	114.0(3)	114.9	114.9(10)
p_{19}	∠SCC(F_3) difference	−0.5(5)	−0.6	−0.6(5)
p_{20}	∠CCF average	111.4(1)	110.6	···
p_{21}	∠CCF difference 1	0.3(5)	0.0	0.0(5)
p_{22}	∠CCF difference 2	2.3(5)	2.7	2.7(5)
p_{23}	∠CCF difference 3	1.5(5)	1.4	1.4(5)
p_{24}	∠CCF difference 4	2.8(5)	2.8	2.8(5)
p_{25}	∠F(3)C(1)F(4)	109.0(9)	108.4	108.4(10)
p_{26}	∠F(5)C(1)F(4)	108.3(9)	108.1	108.1(10)
p_{27}	∠F(17/19)C(15)F(18)	108.2(9)	108.2	108.2(10)
p_{28}	∠CC═O mean	119.5(6)	119.1	119.1(10)
p_{29}	∠H(8)C(7)H(9)	108.2(7)	108.3	108.3(7)
p_{30}	∠H(22)C(21)H(23)	108.3(7)	108.3	108.3(7)
p_{31}	∠SCC(H_3) average	113.1(6)	111.1	···
p_{32}	∠SCC(H_3) difference	3.8(6)	3.5	3.5(6)
p_{33}	ϕF(4)C(1)C(2)S(14)	4.1(41)	16.9	···
p_{34}	ϕC(1)C(2)S(14)C(7)	161.4(27)	173.8	···
p_{35}	ϕC(2)S(14)C(7)C(10)	−78.0(22)	−78.4	−78.4(30)
p_{36}	ϕH(11)C(10)C(7)S(14)	−176.5(51)	−178.1	−178.1(50)
p_{37}	Amount of C_1 conformer	0.49(3)	0.41	···
Dependent				
p_{38}	rC(2)═O(6)	121.6(3)	121.4	···
p_{39}	rC(16)═O(20)	121.6(3)	121.4	···
p_{40}	rC(1)—F(4)	134.1(4)	134.0	···
p_{41}	rC(15)—F(18)	134.1(4)	134.0	···
p_{42}	rC(1)—F(3)	133.6(2)	133.2	···
p_{43}	rC(1)—F(5)	134.4(2)	134.0	···
p_{44}	rC(15)—F(17/19)	134.0(2)	133.6	···
p_{45}	rC(7)—S(14)	182.6(3)	181.5	···
p_{46}	rC(21)—S(28)	182.7(3)	181.6	···
p_{47}	rC(7)—C(10)	153.2(5)	152.5	···
p_{48}	rC(21)—C(24)	153.3(5)	152.6	···
p_{49}	rC(1)—C(2)	154.6(3)	154.6	···
p_{50}	rC(15)—C(16)	154.6(3)	154.6	···
p_{51}	rC(2)—S(14)	176.1(3)	175.2	···
p_{52}	rC(16)—S(28)	175.9(3)	175.0	···
p_{53}	∠CCH(11)	111.8(11)	109.7	···
p_{54}	∠CCH(12)	112.9(11)	110.9	···
p_{55}	∠CCH(13)	112.7(11)	110.7	···
p_{56}	∠CCH(25)	111.5(11)	109.3	···
p_{57}	∠CCH(26/27)	113.5(11)	111.4	···
p_{58}	∠C(2)S(14)C(7)	95.9(6)	97.6	···
p_{59}	∠C(16)S(28)C(21)	95.9(6)	97.4	···
p_{60}	∠CCF(4)	113.1(4)	112.4	···
p_{61}	∠CCF(3)	111.5(4)	110.4	···
p_{62}	∠CCF(5)	110.0(4)	109.0	···
p_{63}	∠CCF(18)	113.1(4)	112.5	···
p_{64}	∠CCF(17/19)	110.3(4)	109.7	···
p_{65}	∠S(14)C(7)C(10)	115.0(6)	112.8	···
p_{66}	∠S(28)C(21)C(24)	111.3(7)	109.3	···
p_{67}	∠S(14)C(2)C(1)	113.7(4)	114.6	···
p_{68}	∠S(28)C(16)C(15)	114.3(4)	115.2	···

$$p_4 = [\mathrm{C}(1/15) — \mathrm{F}(3/5/17/19)_{\mathrm{mean}}] - \{[\mathrm{C}(2/16) = \mathrm{O}(6/20)_{\mathrm{mean}}] + [\mathrm{C}(1/15) — \mathrm{F}(4/18)_{\mathrm{mean}}]\}/2,$$

$$p_5 = [\mathrm{C}(1/15) — \mathrm{F}(4/18)_{\mathrm{mean}}] - [\mathrm{C}(2/16) = \mathrm{O}(6/20)_{\mathrm{mean}}],$$

and the distances were constructed thus

$$[\mathrm{C}(2/16) = \mathrm{O}(6/20)_{\mathrm{mean}}] = p_1 - p_2/6 - p_3/5 - p_4/2 - p_5/5,$$

$$[\mathrm{C}(2/16) — \mathrm{O}(14/28)_{\mathrm{mean}}] = p_1 - p_2/6 - p_3/5 - p_4/2 + p_5/2,$$

$$[\mathrm{C}(1/15) — \mathrm{F}(3/17)_{\mathrm{mean}}] = p_1 - p_2/6 - p_3/5 + p_4/2,$$

$$[\mathrm{C}(1/15) — \mathrm{F}(4/5/18/19)_{\mathrm{mean}}] = p_1 - p_2/6 + 4 \times p_3/5,$$

$$[\mathrm{C}(7/21) — \mathrm{O}(14/28)_{\mathrm{mean}}] = p_1 + 5 \times p_2/6.$$

The mean C—S distances were described by the average of $[\mathrm{C}(2/16)—\mathrm{S}(14–28)_{\mathrm{mean}}]$ and $[\mathrm{C}(7/21)—\mathrm{S}(14/28)_{\mathrm{mean}}]$ and the difference between them ($p_{6–7}$). A single mean C—H parameter (p_8) completed the set of distance parameters used in the model.

Between the two conformers there are five unique C—C—H angles, and these were described as the overall average and a series of four differences,

$$p_9 = \mathrm{CCH}(11)/6 + \mathrm{CCH}(12)/6 + \mathrm{CCH}(13)/6 + \mathrm{CCH}(25)/6 + 2 \times \mathrm{CCH}(26/27)/6,$$

$$p_{10} = [\mathrm{CCH}(11)/3 + \mathrm{CCH}(12)/3 + \mathrm{CCH}(13)/3] - [\mathrm{CCH}(25)/3 + 2 \times \mathrm{CCH}(26/27)/3],$$

$$p_{11} = \mathrm{CCH}(11)/3 - [\mathrm{CCH}(12)/2 + \mathrm{CCH}(13)/2],$$

$$p_{12} = \mathrm{CCH}(12) — \mathrm{CCH}(13),$$

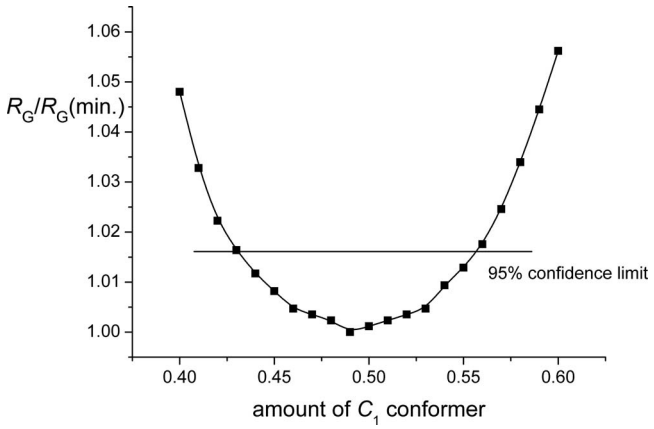

FIG. 5. Proportion of the C_1-symmetric conformer in experimental mixture against R_G/R_G(min). The horizontal line gives an estimate of the uncertainty (2σ) of the value.

$$p_{13} = \mathrm{CCH(25)} - \mathrm{CCH(26/27)},$$

with the individual angles therefore defined as

$$\mathrm{CCH(11)} = p_9 + p_{10}/2 + 2 \times p_{11}/3,$$

$$\mathrm{CCH(12)} = p_9 + p_{10}/2 - p_{11}/3 + p_{12}/2,$$

$$\mathrm{CCH(13)} = p_9 + p_{10}/2 - p_{11}/3 - p_{12}/2,$$

$$\mathrm{CCH(25)} = p_9 - p_{10}/2 + 2 \times p_{13}/3,$$

$$\mathrm{CCH(26/27)} = p_9 - p_{10}/2 - p_{13}/3.$$

Three H—C—H angles (p_{14-16}) relating to the internal angles within the methyl groups were used—two for the C_1 conformer and one for the C_s conformer. As the C(2)—S(14)—C(7) and C(16)—S(28)—C(21) angles were calculated to be almost identical, a single mean value (p_{17}) was used to describe both. The S(14)—C(2)—C(1) and S(28)—C(16)—C(15) angles were described using the average of the two values and the difference between them (p_{18-19}). In a manner identical to that used for the CCH angles, the CCF angles were described using the average of all five and a set of differences (p_{20-24}). Three FCF angles completed the description of the CF_3 groups (p_{25-27}). A mean C—C═O value was used in the model (p_{28}), reflecting the similarity of the calculated values for the two conformers. The methylene groups of the two conformers were described using different H—C—H angles (p_{29-30}). Unsurprisingly, the S(14)—C(7)—C(10) and S(28)—C(21)—C(24) angles were quite different and were therefore described using the average of the two and their difference (p_{31-32}). Finally, the model was completed using four dihedral angles (p_{33-37}) to describe the deviation of the C_1 conformer from C_s symmetry. All 36 independent geometric parameters were refined by least-squares. Restraints were applied, using the SARACEN method,[43] to parameters that could otherwise not be refined (Table III). The restraints were based on values calculated at the MP2/6-311++G(d,p) level, and the uncertainties were derived from the changes in value of each parameter during the series of calculations that was performed. In addition, ten groups of amplitudes of vibration were refined. (See Table S7 for a list of amplitudes of vibration).[20] Finally, the relative amounts of each conformer in the experimental mixture were estimated by changing parameter 37 in a stepwise manner and recording the R factor. Figure 5 shows these R factors plotted in the form R_G/R_G(min) against the amount of C_1 conformer, showing that the best fit to the experimental data occurs with a ratio of C_1 to C_s conformer of approximately 49:51. Using Hamilton's statistical tables,[44] the standard deviation of the amount of each conformer has been estimated by drawing a horizontal line at R_G/R_G(min)=1.016, representing the 95% confidence limit (2σ). This leads to the amount of C_1 conformer, including estimated standard deviation, of 49(3)% and a corresponding difference in energy of 1.79 kJ mol^{-1}, with the C_s conformer lower in energy.

The success of the refinement can be assessed numerically using the final R factor, which was R_G=0.092 (R_D

TABLE IV. Selected GED experimental bond length and hyperconjugation interactions calculated with B3LYP/6-311++G(d,p) to the YSC(O)R moiety. All NBO energies are from B3LYP/6-311++G(d,p) calculations from this work. Distances are in picometer, angles are in degrees, and energies are in kJ mol^{-1}.

	$CF_3C(O)SH$[a]	$CF_3C(O)SCl$[a]	$CF_3C(O)SCH_3$[a]	$CF_3C(O)SCH_2CH_3$[b]	$ClC(O)SCH_2CH_3$[c]	$CH_3C(O)SCH_2CH_3$
rC—S	173.8	176.5	174.3	175.9	175.2	178.6
rS—Y	133.5	201.3	180.7	182.7	180.0	184.5
rC═O	121.7	122.4	120.6	121.6	120.0	121.5
rR—C(O)	152.4	154.6	152.7	154.6	172.5	151.3
∠S—C═O	127.6	126.4	126.1	125.8	127.6[d]	118.2
∠C—S—Y	96.5	99.4	98.1	95.9	103.9	104.7
n(σ)S→σ^*C═O	20.61	17.43	22.36	22.91	27.4	⋯
n(π)S→π^*C═O	132.13	123.64	151.61	153.23	151.1	120.75
Sum nS→π^*C═O	152.74	142.83	174.0	176.14	178.5	120.75
n(σ)O→σ^*C—S	8.78	7.48	7.77	8.19	12.62	6.77
n(π)O→π^*C—S	133.22	150.48	126.19	123.94	102.36	134.4
Sum nO→π^*C—S	141.99	157.96	133.97	132.13	114.99	141.2
Sum total[c]	294.73	299.04	307.94	308.27	293.49	261.95

[a]GED parameters from Ref. 46.
[b]This work.
[c]Experimental geometrical parameters from Ref. 47.
[d]Calculated value.

TABLE V. Frequencies/cm^{-1} and observed bands in the infrared and Raman spectra of $CF_3COSCH_2CH_3$.

Infrared[a]			Raman[b]	Approximate description
Gas	Liquid (RT)	Low temp. (−100 °C)	Liquid	
3005 sh		3005 sh		ν_a CH_2
2995 sh	2995 sh	2995 sh		ν_a CH_3
2989 w (C_s) 2983 w (C_1)	2982 w	2982 m	2981 (31) (C_s) 2979 sh (C_1)	ν_a CH_3
2950 2947 w 2945	2947 sh (C_s) 2942 w (C_1)	2941 m	2942 (100)	ν_s CH_2
2891 w (C_s) 2889 w (C_1)	2886 vw 2884 vw	2885 m	2886 (24)	ν_s CH_3
1724 vs	1709 v (C_s) 1700 sh (C_1)	1705 vs (C_s) 1692 vs (C_1)	1708 (24) (C_s) 1696 sh (C_1)	ν C═O
1461 w		···	1464 sh	δ_a CH_3
1457 w	1457 w	1457 s	1457 (10) (C_s) 1454 (10) (C_1)	δ_a CH_3
1457 w	1420 vw	1418 m	1427 sh (C_s) 1420 (8) (C_1)	δ CH_2
1389 vw	1387 vw (C_s) 1383 vw (C_1)	1391 sh (C_s) 1382 m (C_1)	1390 (2) (C_s) 1384 (2) (C_1)	δ_s CH_3
1339 vvw (C_1) 1337 vvw (C_s)	1338 vvw	1339 w		ω CH_2
1290s	1287 s	1287 vs	1287 (9)	ν_s CF_3
1273 sh	1274 sh (C_s) 1253 sh (C_1)	1274 vs (C_s) 1254 s (C_1)	1273 (6) (C_s) 1253 (3) (C_1)	$\tau\omega$ CH_2
1214 vs	1210 vs	1205 vs	1206 (3)	ν_a CF_3
1187 vs	1164 vs	1158 vs	1171 (2)	ν_a CF_3
1061 sh (C_s) 1056 vvw (C_1)	1060 w (C_s) 1054 sh (C_1)	1062 m	1060 (19)	ρ CH_3
1051 vw	1051 vvw	1051 w	1052 sh	ρ CH_3
995 w	998 w	1000 w	···	ν C(7)—C(10)
			975 (5) (C_s)	
957 vs	956 vs	955 vs	955 (3) (C_1)	ν C(1)—C(2)
800	···	776 w (C_s) 760 m (C_1)	760 (9)	ρ CH_2
749 745 m 741	744 m	744 s	744 (30)	δ_s CF_3
703 vw	695 w	695 m	···	ρ C═O out-of-plane
673 vvw (C_s) 664 vvw (C_1)	668 vw	683 w (C_s) 664 w (C_1)	685 (10) (C_s) 664 (35) (C_1)	ν C(2)═S(14)
597w (C_1) 591w (C_s)	595 m	595 s	596 (14)	ν S—C(7)
533 w	546 sh (C_s) 538 vvw (C_1)	547 sh (C_s) 539 m (C_1)	538 (14)	δ_a CF_3
511 vw	510 vvw	511 m	···	δ_a CF_3
			404 (13)	ρ C═O in-plane
			371 sh (C_1) 360 (9) (C_s)	δ C(2)S(14)C(7)
			313 (13) (C_1) 295 (13) (C_s)	δ S(14)C(7)C(10)
			262 (3) (C_1) 250 (4) (C_s)	ρ CF_3
			220 (14)	ρ CF_3
			210 sh	τ CH_3
			125 (2)	δ C(1)C(2)S(14)
			98 (16)	τ S(14)C(10)

[a]sh: shoulder; s: strong; w: weak; m: medium; and v: very.
[b]Relative band heights in parentheses.

=0.053), and visually using the goodness of fit of the radial-distribution and difference curves, as seen in Fig. 6, and the molecular-scattering intensity curves (Fig. S3).[20] The least-squares correlation matrix is given in Table S8 (Ref. 20), and coordinates for the final GED structures and for the calculated structures [MP2/6-311++G(d,p)] are given in Tables S9 and S10, respectively.[20]

To allow comparison of the experimental geometrical parameters and conformation of $CF_3CO_2CH_2CH_3$ (Ref. 5) with those for $CF_3COSCH_2CH_3$, we present selected parameters in Table I. In addition, NBO analysis was performed to quantify and compare the role of electron delocalization and the geometrical parameters in each compound.

Replacing the single-bonded oxygen atom in the acetate by sulfur leads to an increase in the C(16)—O(20) and C(21)—C(24) bond lengths, which can be explained by a decrease of 77 kJ mol^{-1} of the lp S/O(14/28) $\rightarrow \sigma^*$C(2/16)—O(6/20) interactions and by 3.38 kJ mol^{-1} of the lp S/O(14/28) $\rightarrow \sigma^*$C(7/21)—C(10/24) interactions in the thioacetate. There is a slight increase in the C(15)—C(16)—S/O(28) angle, but the C(16)—S/O(28)—C(21) angle is of course much narrower in the thioacetate, having sulfur instead of oxygen as the central atom. The C(16)—S/O(28)—C(21)—C(24) dihedral angle is much smaller in the *gauche* conformer of the thioacetate than in the corresponding conformer of the acetate.

The differences in the molecular structure of thioesters and oxoesters and their relation with the hyperconjugative interaction have been confirmed by Erben *et al.*,[45] who observed that the hyperconjugative interaction is "less important when the donor lone pair is formally located at the sulfur atom rather than at the oxygen atom" It is interesting to compare the effects of the substitution of both trifluoro and ethyl groups on the R—C(O)S—Y moiety. In Table IV we present selected parameters and hyperconjugative interactions for $CF_3C(O)SH$,[46] $CF_3C(O)SCl$,[46] $CF_3C(O)SCH_3$,[46] $CF_3C(O)SCH_2CH_3$, $ClC(O)SCH_2CH_3$,[47] and

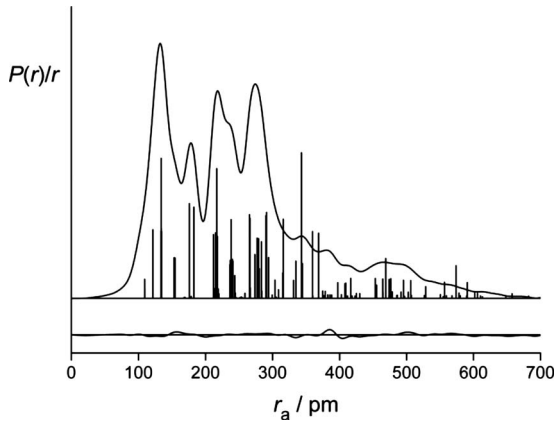

FIG. 6. Experimental radial-distribution curve and theoretical-minus-experimental difference curve for the refinement of $CF_3COSCH_2CH_3$. Before Fourier inversion the data were multiplied by $s\exp(-0.000\,02s^2)/(Z_O-f_O)(Z_F-f_F)$.

$CH_3C(O)SCH_2CH_3$. We are studying the last molecule at the moment and the data used here are results of the theoretical calculations and from the paper of Nagy *et al.*[48,49]

When we analyze the replacement of the trifluoro group by a less electronegative group such as CH_3 or Cl, a decrease in the C—S bond length is observed, which can be explained by an increase in the anomeric effect, as seen for $lp\sigma O \rightarrow \sigma^*C—S$ and $lp\sigma S \rightarrow \sigma^*C=O$ in $ClC(O)SCH_2CH_3$.[47]

If we compare the sums of individually determined effects for Y=H, CH_3, and CH_2CH_3 we observe an increase in the delocalization as the chain length increases. The chlorine atom is a special case, as it has a greater electronegativity compared to the other substituents; this results in a decrease in the electronic delocalization in the R—C(O)S—Y moiety.

A. Vibrational study

The details of the IR (gas, liquid, and solid) and Raman spectra, together with a tentative assignment, are collected in Table V. Representative spectra are illustrated in Fig. 7 (IR spectra of the gas, liquid, and solid) and Fig. 8 (calculated and experimental Raman spectra).

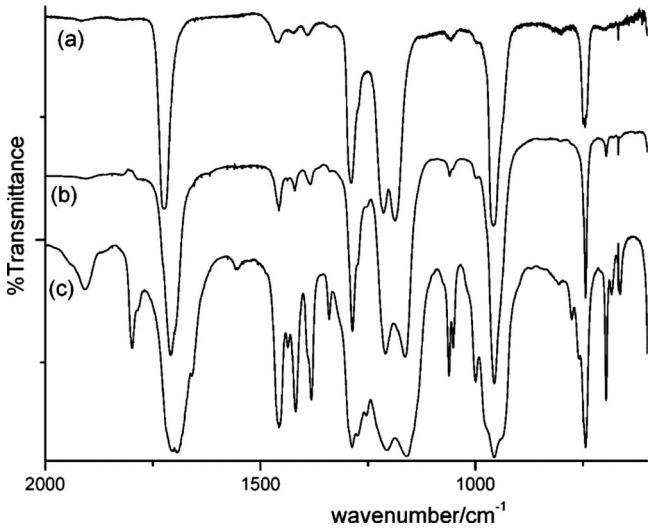

FIG. 7. Infrared spectra in (a) the gas phase (path length of 10 cm, 5 torr), (b) the liquid phase (room temperature), and (c) the solid phase of $CF_3COSCH_2CH_3$ (resolution: 1 cm^{-1}).

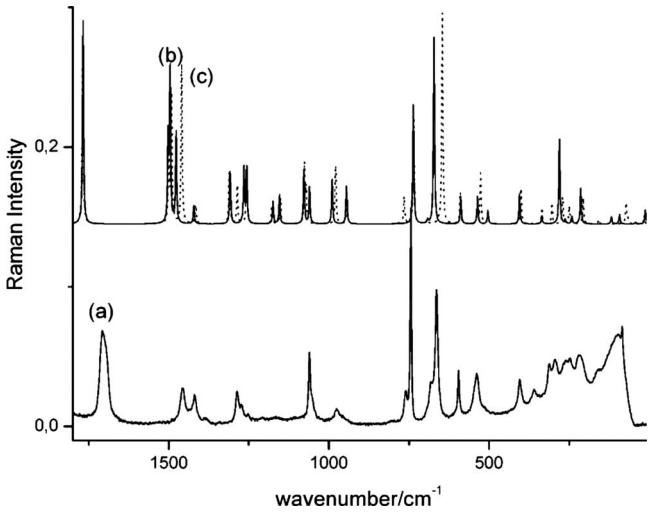

FIG. 8. Infrared and Raman spectra of liquid $CF_3COSCH_2CH_3$ at room temperature.

The calculated wavenumbers for the 36 normal modes of vibration of $CF_3COSCH_2CH_3$ (22 A′ and 14 A″) for the C_s conformer appear in Table VI, where they are compared with the measured values. The assignment of the experimental bands was made after comparison with related molecules and with the results of the calculations.

DFT calculations reproduced the normal wavenumbers of vibrations with the following RMSDs for each basis set: 65 cm^{-1} for 6-31G(d), 56 cm^{-1} for 6-311G(d,p), and 53 cm^{-1} for 6-311++G(d,p). The results with the combination B3LYP/6-311++G(d,p) were used for the vibrational analysis to facilitate the comparison of the present results with those obtained previously for related molecules. At room temperature, most bands are attributable to the same fundamental for both conformations. The IR (gas, liquid, and solid) and Raman spectra demonstrate the presence of conformers of C_s and C_1 symmetry by the resolution of several fundamental modes of vibration.

The bands at 2942 and at 2886 cm^{-1} in the Raman spectrum are assigned to the symmetric modes of the methylene and methyl groups, respectively. These bands are split into two components in the liquid and gas IR spectra, showing the presence of the two conformers (see Table V).

The carbonyl band is extremely sensitive to the conformers present in the liquid and solid phases. In the gas phase we observed only one band at 1724 cm^{-1}. The pair of strong bands at 1709–1702 and 1700–1692 cm^{-1} in the liquid and solid infrared spectra is assigned to the CO stretching mode for C_s and C_1 conformers, respectively (see Table V). The calculated values for both conformers are 1769 cm^{-1} (C_1) and 1768 cm^{-1} (C_s).

B. Calculation of force constants

The force field in Cartesian coordinates, as generated by the Gaussian program, was transformed to the set of nonredundant natural coordinates defined in Table S11.[20] Such co-

TABLE VI. Observed and calculated frequencies/cm^{-1}, infrared and Raman intensity, and potential-energy distribution for $CF_3COSCH_2CH_3$.

Mode	Observed	Calculated[a]	Calculated SQM[b]	IR intensity[c]	Raman activity[d]	Potential-energy distribution
A′						
1	2995	3101	2985	16.74	108.20	97 S_1
2	2947	3075	2983	2.77	81.72	98 S_2
3	2891	3036	2893	18.95	190.16	100 S_3
4	1724	1768	1729	298.35	14.15	100 S_4
5	1461	1503	1479	4.80	6.03	100 S_5
6	1457	1478	1446	4.01	6.31	90 S_6+9 S_{28}
7	1389	1422	1373	4.77	1.29	98 S_7
8	1339	1308	1340	37.12	3.66	92 S_8
9	1290	1256	1277	105.81	3.86	40 S_9+30 S_{12}+30 S_{14}
10	1214	1174	1211	240.10	1.56	93 S_{10}+10 S_{17}
11	1061	1078	1064	11.26	3.82	45 S_{11}+34 S_{13}
12	995	989	977	4.46	3.22	26 S_9+11 S_{12}+11 S_{29}+24S_{16}+35 S_{18}
13	957	944	955	306.58	2.65	28 S_{28}+47 S_{13}
14	745	736	754	43.79	8.49	32 S_9+38 S_{14}
15	673	672	659	1.51	12.91	63 S_{15}+6 S_{28}+8 S_{19}+9 S_{32}
16	597	588	593	4.50	1.92	27 S_{15}+16 S_{31}+6 S_{27}+7 S_{12}+8 S_{14}
17	533	536	540	5.63	2.00	35 S_{16}+37 S_{17}
18	404	405	413	0.41	2.05	11 S_{12}+12 S_{16}+24 S_{17}+15 S_{18}+13 S_{19}
19	360	335	344	3.39	0.57	23 S_{18}+38 S_{19}+10 S_{20}+9 S_{32}
20	295	281	284	1.43	5.86	11 S_{12}+15 S_{17}+23 S_{19}+31 S_{20}
21	220	215	221	7.68	2.52	92 S_{12}
22	125	118	121	0.37	0.51	20 S_{18}+30 S_{33}+50 S_{22}
A″						
23	3005	3132	3009	9.86	21.22	80 S_{23}+20 S_{24}
24	2989	3101	2983	9.59	77.61	20 S_{23}+80 S_{24}
25	1457	1496	1453	10.34	10.91	88 S_{25}
26	1273	1265	1255	0.021	3.86	63 S_{26}+18 S_{28}
27	1187	1154	1191	300.91	2.00	100 S_{27}
28	1051	1060	1048	0.01	2.52	34 S_{26}+35 S_{28}+27 S_{13}
29	776	782	773	3.07	0.06	40 S_{28}+60 S_{29}
30	703	692	714	3.18	0.28	51 S_{30}+20 S_{12}
31	511	504	521	3.95	0.91	11 S_{30}+80 S_{31}
32	250	262	263	2.49	0.28	26 S_{31}+67 S_{32}
33	210	242	216	0.63	0.52	23 S_{28}+21 S_{33}+33 S_{14}
34	98	93	83	0.72	0.68	82 S_{34}
35	31	43	31	0.19	0.13	100 S_{35}
36	10	13	11	0.22	0.97	100 S_{36}
RMSD		50.18	9.55			

[a]B3LYP/6-311++G(d,p) calculation; observed and calculated values in cm^{-1}.
[b]From scaled quantum mechanics force field (see text for further definition).
[c]Units are km mol^{-1}.
[d]Units are $Å^4$ amu^{-1}.

ordinates take into account the local symmetry around the C and S atoms and follow the proposals of Fogarasi *et al.*[33] The resulting force field was subsequently scaled using the scheme proposed by Pulay *et al.*,[35] and the initial scale factors were defined using unity for all modes, as shown in Table S12.[20] These scale factors were subsequently refined by the nonlinear least-squares procedure to fit the experimental frequencies.

The refined scale factors corresponding to each force constant appear in Table S12,[20] while the resulting frequencies, RMSD final value, and the potential-energy distribution are reported in Table VI. It can be seen that only half the modes have a participation of $\geq$50% of a single coordinate, whereas other modes represent very complex vibrations in which several coordinates are involved. The SQM force field (Table S13) (Reg. 20) was used to calculate the internal force constants appearing in Table VII, which are in good agreement with the equivalent values for $CF_3CO_2CH_2CH_3$, $CF_3CO_2CH_2CF_3$ and $CF_3SO_2OCH_2CH_3$.[50]

V. CONCLUSIONS

The optimized molecular geometry and conformation for *S*-ethyl trifluorothioacetate have been calculated using MP2 and DFT calculations with different basis sets. At the B3LYP/6-311++G(d,p) level the free energies for the two conformers show that the C_s-symmetric conformer was lower in energy than the C_1 conformer by approximately 2.6 kJ mol^{-1}. NBO calculations have been performed in order to justify the preferred conformation of

TABLE VII. Force constants in internal (valence) coordinates for $CF_3COSCH_2CH_3$ and related molecules.

Force constants[a]	$CF_3COSCH_3CH_2$[b]	$CF_3CO_2CH_2CH_3$[c]	$CF_3CO_2CH_2CF_3$[d]	$CF_3SO_2OCH_2CH_3$[e]
k_f [C(15)—F]	6.28	6.45	6.41	5.93
k_f [C(15)—C/S(16)]	3.49	3.86	3.91	3.11
k_f [C(21)—C(24)]	4.30	4.67	4.53	4.27
k_f [C=O]	12.49	13.13	13.43	···
k_f [C/S(16)—S/O(28)]	2.97	6.42	6.22	5.04
k_f [S/O(28)—C(21)]	2.55	3.96	4.72	4.20
k_f [C(21)—H]	4.88	4.88	5.00	4.90
k_f [C(24)—H]	4.82	4.88	···	4.84
k_f [H—C(21)—H]	0.45	0.50	0.48	0.49
k_f [S/O(28)—C/S(16)=O(20)]	0.70	0.69	0.91	1.27
k_f [C(15)—C/S(16)—S/O(28)]	0.66	0.78	0.72	1.13
k_f [C(15)—C/S(16)=O(20)]	0.70	0.67	0.67	1.04
k_f [C—F/C—F]	0.91	0.93	0.75	0.72

[a]Units are mdyn $Å^{-1}$ for stretches and stretch-stretch interactions and mdyn Å rad^{-2} for angle bends.
[b]This work.
[c]Reference 5.
[d]Reference 6.
[e]Reference 50.

$CF_3COSCH_2CH_3$. We conclude that the electrostatic and steric contributions included in the Lewis term tend to promote the *anti*, *anti* conformer, whereas the delocalization contribution tends to favor the *anti*, *gauche* conformer, as expected from the anomeric effect.

IR and Raman spectra were recorded for $CF_3COSCH_2CH_3$, for which 34 out of the expected 36 normal modes of vibration have been assigned. Both conformers were observed in the IR and Raman spectra. It was possible to scale the theoretical force field by taking the observed frequencies as a basis. The resulting SQM force field served to calculate the potential-energy distribution, which revealed the physical nature of the molecular vibrations. The force constants in internal coordinates were similar to those obtained earlier for related chemical species.

ACKNOWLEDGMENTS

We acknowledge the help of research grants from CIUNT (Consejo de Investigaciones de la Universidad Nacional de Tucumán) and CONICET (Consejo Nacional de Investigaciones Científicas y Técnicas) under Grant No. PIP 112-200801-00629. We thank the EPSRC for funding D.A.W. (Grant No. EP/F037317) and the NSCCS for computational resources.

[1] D. Xu, K. Prasad, A. Repic, and T. J. Blacklock, Tetrahedron Lett. **36**, 41 (1995).
[2] E. E. Schallenberg and M. Calvin, J. Am. Chem. Soc. **77**, 2779 (1955).
[3] N. S. True, C. J. Silvia, and R. K. Bohn, J. Phys. Chem. A **85**, 1132 (1981).
[4] M. E. Defonsi Lestard, M. E. Tuttolomondo, E. L. Varetti, D. A. Wann, H. E. Robertson, D. W. H. Rankin, and A. Ben Altabef, "Gas-phase structure and new vibrational study of methyl trifluoroacetate, $CF_3C(O)OCH_3$," J. Raman Spectrosc. (in press).
[5] M. E. Defonsi Lestard, M. E. Tuttolomondo, E. L. Varetti, D. A. Wann, H. E. Robertson, D. W. H. Rankin, and A. Ben Altabef, "Experimental and theoretical structure and vibrational analysis of ethyl trifluoroacetate, $CF_3CO_2CH_2CH_3$," J. Raman Spectrosc. (in press).
[6] M. E. Defonsi Lestard, M. E. Tuttolomondo, E. L. Varetti, D. A. Wann, H. E. Robertson, D. W. H. Rankin, and A. Ben Altabef, J. Mol. Struct. **917**, 183 (2009).
[7] W. Yang and D. G. Drueckhammer, J. Am. Chem. Soc. **123**, 11004 (2001).
[8] S. E. Ulic, C. O. Della Védova, A. Hermann, H.-G. Mack, and H. Oberhammer, Inorg. Chem. **41**, 5699 (2002).
[9] Q. Shen and K. Hagen, J. Mol. Struct. **128**, 41 (1985).
[10] R. M. Romano, C. O. Della Védova, A. J. Downs, H. Oberhammer, and S. Parsons, J. Am. Chem. Soc. **123**, 12623 (2001).
[11] H.-G. Mack, H. Oberhammer, and C. O. Della Védova, J. Phys. Chem. **95**, 4238 (1991).
[12] H.-G. Mack, C. O. Della Védova, and H. Oberhammer, J. Phys. Chem. **96**, 9215 (1992).
[13] S. E. Ulic, A. Kosma, C. O. Della Védova, H. Willner, and H. Oberhammer, J. Phys. Chem. **110**, 10201 (2006).
[14] M. F. Erben, C. O. Della Védova, H.-G. Mack, H. Oberhammer, and R. Boese, Inorg. Chem. **44**, 7070 (2005).
[15] A. Hermann, S. E. Ulic, C. O. Della Védova, H. Willner, and H. Oberhammer, J. Fluorine Chem. **112**, 297 (2001).
[16] C. M. Huntley, G. S. Laurenson, and D. W. H. Rankin, J. Chem. Soc. Dalton Trans. **1980**, 954.
[17] H. Fleischer, D. A. Wann, S. L. Hinchley, K. B. Borisenko, J. R. Lewis, R. J. Mawhorter, H. E. Robertson, and D. W. H. Rankin, J. Chem. Soc. Dalton Trans. **2005**, 3221.
[18] S. L. Hinchley, H. E. Robertson, K. B. Borisenko, A. R. Turner, B. F. Johnston, D. W. H. Rankin, M. Ahmadian, J. N. Jones, and A. H. Cowley, J. Chem. Soc. Dalton Trans. **2004**, 2469.
[19] A. W. Ross, M. Fink, and R. Hilderbrandt, *International Tables for Crystallography*, edited by A. J. C. Wilson (Kluwer Academic, Dordrecht, 1992), Vol. C, p. 245.
[20] See EPAPS supplementary material at http://dx.doi.org/10.1063/1.3267633 for experimental parameters from the GED refinement, RMSDs between experimental (GED) and calculated geometry data of C_1 and C_s conformers, contributions of Lewis energy hyperconjugation energy, important hyperconjugative interactions, electrostatic contributions to the energies, energies and occupancies of the NBOs, refined and calculated amplitudes of vibration and associated correction values GED refinement, least-squares correlation matrix, GED-determined coordinates, calculated coordinates, definition of natural internal coordinates, scale factors for the force field, SQM force constant matrix, dependence of the relative total energy on the CSCC rotation angle, dependence of attractive and repulsive energy increments on the CSCC dihedral angle, and molecular-scattering intensity curves.
[21] National Service for Computational Chemistry Software (NSCCS), URL: http://www.nsccs.ac.uk.
[22] M. J. Frisch, G. W. Trucks, H. B. Schlegel *et al.*, GAUSSIAN 03, Revision C.02, Gaussian, Inc., Wallingford CT, 2004.
[23] C. Møller and M. S. Plesset, Phys. Rev. **46**, 618 (1934).
[24] R. Krishnan, J. S. Binkley, R. Seeger, and J. A. Pople, J. Chem. Phys. **72**, 650 (1980).

[25] A. D. McLean and G. S. Chandler, J. Chem. Phys. **72**, 5639 (1980).
[26] M. J. Frisch, J. A. Pople, and J. S. Binkley, J. Chem. Phys. **80**, 3265 (1984).
[27] W. J. Hehre, P. R. Schleyer, and J. A. Pople, *Ab Initio Molecular Orbital Theory* (Wiley, New York, 1986).
[28] A. D. Becke, J. Chem. Phys. **98**, 5648 (1993).
[29] C. Lee, W. Yang, and R. G. Parr, Phys. Rev. B **37**, 785 (1988).
[30] J. P. Perdew, K. Burke, and M. Ernzerhof, Phys. Rev. Lett. **77**, 3865 (1996); **78**, 1396(E) (1997).
[31] V. A. Sipachev, J. Mol. Struct.: THEOCHEM **121**, 143 (1985); J. Mol. Struct. **567–568**, 67 (2001).
[32] E. D. Glendening, J. K. Badenhoop, A. D. Reed, J. E. Carpenter, and F. F. Weinhold, *Theoretical Chemistry Institute* (University of Wisconsin, Madison, WI, 1996).
[33] G. Fogarasi, X. Zhou, P. W. Taylor, and P. Pulay, J. Am. Chem. Soc. **114**, 8191 (1992).
[34] E. B. Wilson, J. C. Decius, and P. C. Cross, *Molecular Vibrations* (McGraw-Hill, New York, 1955).
[35] P. Pulay, G. Fogarasi, G. Pongor, J. E. Boggs, and A. Braga, J. Am. Chem. Soc. **105**, 7037 (1983).
[36] W. B. Collier, Program FCARTP (QCPE #631), Department of Chemistry, Oral Roberts University, Tulsa, OK (1992).
[37] B. Nielsen and A. J. Holder, GAUSSVIEW, User's Reference, Gaussian, Inc., Pittsburgh, PA (1997).
[38] M. E. Tuttolomondo, A. Navarro, T. Peña Ruiz, E. L. Varetti, S. A. Hayes, D. A. Wann, H. E. Robertson, D. W. H. Rankin, and A. Ben Altabef, J. Phys. Chem. A **111**, 9952 (2007).
[39] J. L. Duncan, Mol. Phys. **28**, 1177 (1974).
[40] S. Millefiori and A. Alparone, J. Chem. Soc., Faraday Trans. **94**, 25 (1998).
[41] L. Radom, W. J. Hehre, and J. A. Pople, J. Am. Chem. Soc. **94**, 2371 (1972).
[42] L. Radom and J. A. Pople, J. Am. Chem. Soc. **92**, 4786 (1970).
[43] A. J. Blake, P. T. Brain, H. McNab, J. Miller, C. A. Morrison, S. Parsons, D. W. H. Rankin, H. E. Robertson, and B. A. Smart, J. Phys. Chem. **100**, 12280 (1996); P. T. Brain, C. A. Morrison, S. Parsons, and D. W. H. Rankin, J. Chem. Soc. Dalton Trans. **1996**, 4589; N. W. Mitzel and D. W. H. Rankin, *ibid.* **2003**, 3650.
[44] W. C. Hamilton, Acta Crystallogr. **18**, 502 (1965).
[45] M. F. Erben, R. Boese, C. O. Della Védova, H. Oberhammer, and H. Willner, J. Org. Chem. **71**, 616 (2006).
[46] K. I. Gobbato, C. O. Della Védova, H. G. Mack, and H. Oberhammer, Inorg. Chem. **35**, 6152 (1996).
[47] S. E. Ulic, E. M. Coyanis, R. M. Romano, and C. O. Della Védova, Spectrochim. Acta, Part A **54**, 695 (1998).
[48] P. I. Nagy, F. R. Tejada, J. G. Sarver, and W. S. Messer, J. Phys. Chem. A **108**, 10173 (2004).
[49] B. J. Lynch and D. G. Truhlar, J. Phys. Chem. A **105**, 2936 (2001).
[50] M. E. Tuttolomondo, A. Navarro, E. L. Varetti, and A. Ben Altabef, J. Raman Spectrosc. **36**, 427 (2005).